Are Deep Sequence Classifiers Good at Non-Trivial Generalization?

Francesco Cazzaro
Universitat Politècnica de Catalunya,
Barcelona, Spain
`{francesco.cazzaro,`

Ariadna Quattoni
Universitat Politècnica de Catalunya,
Barcelona, Spain
`ariadna.julieta.quattoni}@upc.edu`

Xavier Carreras
dMetrics,
Brooklyn, NY

Abstract

Recent advances in deep learning models for sequence classification have greatly improved their classification accuracy, specially when large training sets are available. However, several works have suggested that under some settings the predictions made by these models are poorly calibrated. In this work we study binary sequence classification problems and we look at model calibration from a different perspective by asking the question: Are deep learning models capable of learning the underlying target class distribution? We focus on sparse sequence classification, that is problems in which the target class is rare and compare three deep learning sequence classification models. We develop an evaluation that measures how well a classifier is learning the target class distribution. In addition, our evaluation disentangles good performance achieved by mere compression of the training sequences versus performance achieved by proper model generalization. Our results suggest that in this binary setting the deep-learning models are indeed able to learn the underlying class distribution in a non-trivial manner, i.e. by proper generalization beyond data compression.

1 Introduction

Recent advances in deep learning models for sequence classification have greatly improved their classification accuracy, specially when large training sets are available. However, several works have suggested that under some settings the predictions made by these models are poorly calibrated: a model might provide in general correct predictions but give bad estimates of the confidence scores $\Pr(y|x)$. Having well calibrated estimates of $\Pr(y|x)$ is crucial to many machine learning applications. For example, this is critical in systems in which an end user needs to make a decision based on the prediction of the model. Here a good estimate is as important as a good prediction.

In this work we study binary sequence classification with a focus on sparse sequence classification tasks in which only a very small fraction of the sequences in the domain belong to the target class. These types of problems naturally arise in several applications, for example in NLP or in Computational Biology where distinguishing relevant segments in DNA sequences is challenging as it is postulated that only about 1–3% of segments have any biological significance [Eskin, 2002].

While traditional evaluations on model calibration have focused on the quality of the conditional prediction $\Pr_M(y|x)$ in this paper we look at model evaluation from a different perspective by asking the question: Are deep learning models capables of learning the underlying target distribution? The main idea is quite simple, if we have access to large quantities of unlabeled data that accurately represent the input distribution we can estimate the joint distribution $\Pr_M(y, x)$ implicitly induced by the conditional model and then we can compare it to the true distribution.

Workshop on Robustness in Sequence Modeling, 36th Conference on Neural Information Processing Systems (NeurIPS 2022).

We conduct experiments using three deep-learning models: an RNN, a Transformer and a WFA (i.e. Weighted Finite Automata, a form of RNN with linear activation). Our results suggest that in the binary classification setting the deep-learning models are indeed able to learn the underlying class distribution in a non-trivial manner. These results seem to be consistent with previous studies showing that deep-learning models provide calibrated predictions for binary classification problems [Niculescu-Mizil and Caruana, 2005]. Our main contributions are: 1) We present a novel evaluation framework for sequence prediction models. By exploiting unlabeled data, we evaluate the model with respect to the implicitly induced joint distribution. 2) Our evaluation distinguishes performance over components of the distribution seen in training data as well as unseen components explicitly differentiating compression from generalization. 3) Our experiments on a sparse sequence classification task show that deep learning architectures are able to induce good distributions in a non-trivial manner.

2 Related Work

In the recent literature several works have addressed the problem of model calibration. Some of these studies have shown that for some deep learning architectures, the predictions produced by the models are not well calibrated [Guo et al., 2017] [Kumar and Sarawagi, 2019] especially for non pre-trained transformers [Desai and Durrett, 2020]. In contrast, for the case of binary classification some previous work has suggested that they are indeed well calibrated [Niculescu-Mizil and Caruana, 2005]. To our knowledge we are the first ones to study calibration by looking at the joint distribution $\Pr(x, y)$ induced by the learned classifier instead of the quality of the conditional class predictions.

Calibration aside, several works have compared the classification performance of different deep-learning architectures: CNNs and RNNs [Józefowicz et al., 2016] [Yin et al., 2017], Transformers and RNNs [Karita et al., 2019] [Lakew et al., 2018], Transformers and CNNs [Kolesnikov et al., 2021] [Pinto et al., 2021] [Bai et al., 2021], WFA to CNNs [Quattoni and Carreras, 2020] and WFA to RNNs [Quattoni and Carreras, 2019].

Finally, an orthogonal related problem is that of developing deep learning models for density estimation. These include Transformers [Fakoor et al., 2020], Autoregressive Networks [Uria et al., 2016] [Oliva et al., 2018] and Flow Models [Durkan et al., 2019] [De Cao et al., 2020].

3 Evaluating Deep-Learning Model as Moment Predictors

Our goal is to evaluate models defined over sequences of discrete symbols. More precisely we consider an alphabet Σ and the set of all possible sequences $\Sigma^\star$. In general, we can think of probabilistic binary sequence classifiers as functions from $\Sigma^\star \to [0, 1]$. In our setting we assume that we have access to a large set of sequences $U = \{x^{(1)}, \ldots, x^{(u)}\}$ sampled according to the underlying distribution over $\Sigma^\star$. We can think of U as a large set of unlabeled sequences that represent the domain of the sequence classification task. The target class Y that we wish to learn is a subset of sequences in U, that is $Y \subset U$. We are particularly interested in cases where the target class is rare, that is cases in which $|Y|$ is significantly smaller than $|U|$.

We will create a labeled training set $T = \{(x^{(1)}, y^{(1)}), \ldots, (x^{(m)}, y^{(m)})\}$ of size m by sampling sequences from U and labeling $y = 1$ as positive instances if they appear in Y, and otherwise as negative instances $y = 0$. Section 4 contains further details about how we create the task data from an existing dataset, for various training sizes m. Given a training set we will train a sequence classifier M that defines a distribution $\Pr_M(y|x)$.

In this work, we consider three sequence classification models: an **RNN**, a **Transformer** and a **WFA**. As recurrent neural network (RNN) we employ a multi-layer LSTM [Hochreiter and Schmidhuber, 1997] with a binary classification feed-forward layer on top. For the Transformer we select the BERT [Devlin et al., 2019] architecture, we don't use the pre-trained weights and we expand the embeddings with new randomly initialized ones to deal with the protein dataset vocabulary. Both models output the conditional probability $\Pr(l|x)$ where x is a sentence and l a label. We also evaluate a WFA (Weighted Finite Automata; which in essence is an RNN with linear activation functions [Rabusseau et al., 2019]) employing the ensemble proposed in Quattoni and Carreras [2020].

3.1 Evaluation Metrics

The sequence model M that we wish to evaluate defines a conditional distribution $\Pr_M(y|x)$. Generally, we would like to compute the true error of M by evaluating the model on the true distribution $\Pr(x, y)$. In this section, we will use the set U as a proxy for $\Pr(x)$, and specifically we will estimate the *moments* of M on the joint distribution $\Pr_M(x, y)$ that is implicitly induced by the model over the target class.[1] More precisely, consider the set:

$$Z_n = \{z_n \mid z_n \in \Sigma^n, \exists x \in U \text{ such that } z_n \in x\} \tag{1}$$

where z_n is a sub-sequence of size n, $z_n \in x$ indicates that z_n is a sub-sequence of a domain sequence x, and therefore Z_n is the set of all sub-sequences of size n observed in U. We use these sub-sequences as the support set to compute moments of a model, and we define the *moment* function $E_M : z_n \times U \to \mathbb{R}$ as:

$$E_M(z_n, U) = \frac{1}{|U|} \sum_{x \in U} \Pr_M(y|x)\ \#[z_n \in x] \tag{2}$$

where z_n is a sub-sequence of length n and $\#[z_n \in x]$ is a function that counts the number of times that z_n appears in sequence x. From now on, we will assume a fixed U and drop it from the expression, and we will refer to the sub-sequences z_n and their values $E_M(z_n)$ as the *moments* of M. Since we assume that U is a good representation of the the domain, $E_M(z_n)$ can be regarded as an estimate of the expected number of times that we should observe z_n in a sample from $\Pr_M(x, y)$.

Given sets U and Y, the *moments* from the true joint distribution $\Pr_Y(x, y)$ can be computed similarly as:

$$E_Y(z_n) = \frac{1}{|U|} \sum_{x \in Y} \#[z_n \in x] \tag{3}$$

Putting it all together, if we have a domain represented by a set of unlabeled sequences U, a subset of target sequences Y and a model $\Pr_M(y|x)$, we can compute the model's *moment* function $E_M(z_n)$ and compare it to the true *moments* $E_Y(x_n)$. Notice that for a model that learns the target class perfectly (i.e. a model that gives accurate predictions and that it is perfectly calibrated) we will have $E_M(z_n) = E_Y(z_n)$ for all *moments* in N.

Now that we have the necessary functions, we propose to evaluate a model M by comparing E_M and E_Y. To compare the *moment* functions we propose the following metrics:

MSPC: This metric measures the Spearman rank correlation between gold and model *moments* of a fixed length. The Spearman correlation coefficient measures the strength and direction of association between ranked variables. In our evaluation a high MSPC means that the model sorts the *moments* of the distribution in a way that is similar to the gold ordering. The MSPC is computed as:

$$\frac{\operatorname{cov}(\operatorname{rank}[E_M(z_n)], \operatorname{rank}[E_Y(z_n)])}{\sigma(\operatorname{rank}[E_M(z_n)]) \cdot \sigma(\operatorname{rank}[E_Y(z_n)])} \tag{4}$$

where $\operatorname{rank}[E(z_n)]$ are the raw function scores for all $z_n \in Z_n$ converted to ranks. In essence, this metric measures the agreement on partial orderings induced by the model and gold *moment* functions. That is, given any two pairs of *moments* of a fixed length z_n and z'_n whenever $E_Y(z_n) > E_Y(z'_n)$ we want $E_M(z_n) > E_M(z'_n)$.

MSPCP: While MSPC is a useful metric when evaluating the class distribution induced by a model, we need to keep in mind that for longer *moments* $E_Y(z_n)$ will be sparse and for most inputs it will be 0 since we are targeting a rare class. So in this context we compute the Spearman rank correlation between gold non-zero *moments* and the model prediction for those *moments*, this will give an idea of how well the model would sort the *moments* of the target distribution if it knew the true support of the target *moments* function.

MR: as MSPC might be overly harsh, a complementary alternative metric in this case is the mean-rank given to the target non-zero *moments*:

$$1 - \sum_{z_n \,:\, E_Y(z_n) > 0} \frac{\operatorname{rank}[E_M(z_n)]}{|Z_n|} \tag{5}$$

[1]We highlight that the set U is assumed to be sampled from the true $\Pr(x)$ and will contain repetitions of each distinct x proportional to its likelihood. And so does Y. This detail is relevant because we can think of U as an empirical estimate of $\Pr(x)$, which is necessary for the definitions of moments in this section.

This metric captures how well a model performs in the task of making the binary prediction of which *moments* should be non-zero for the target class.

We believe that it is important to make a distinction between the ability of a model to compress data versus its ability to generalize to unseen data. A natural way to achieve this goal is to make a distinction between *moments* that have been seen in the training set, versus *moments* that have not been seen. That is, for any training set T and *moment* length n we can define a subset $Z_n^T \subseteq Z_n$:

$$Z_n^T = \{z_n \in Z_n : z_n \text{ appears in } T\} \tag{6}$$

Given training set T we can define its analogous *unseen* evaluation by computing the metric over $Z_n \setminus Z_n^T$. We call these new metrics: **MSPC-U**, **MSPCP-U** and **MR-U**.

In order to evaluate the generalization ability of a model we will also consider a baseline model that memorizes the training data and makes predictions with the observed training *moments*. More precisely, given a training set T the baseline will compute the *moments* function as:

$$E_{B_T}(z_n) = \frac{1}{|U|} \sum_{(x,y)\in T:y=1} \#[z_n \in x] \tag{7}$$

4 Experiments

To generate the data used in our experiments we use the PFAM dataset [El-Gebali et al., 2018]. This dataset consists of aminoacid sequences pertaining to different protein families. Deep-models have been shown to be very successful at classifying the complete sequences [Bileschi et al., 2019] [Szalkai and Grolmusz, 2018]. To derive a more challenging task we decide to work with segments and we generate the unlabeled set U by sampling sequence segments of size 5.

To create our target class Y we pick a protein-family and select all segments that appear in sequences from that family. We select as our target the most rare or sparse family based on the ratio $|Y|/|U|$. We also select a second family as validation data. We create 5 labeled training sets $T = \{(x^{(1)}, y^{(1)}), \dots, (x^{(m)}, y^{(m)})\}$ by sampling sequences with $m \in \{400, 1000, 2000, 4000, 8000\}$. For the optimization details refer to appendix A.

4.1 Results

To summarize the results, for each training set size and model, we compute an aggregate metric, which we refer as MICRO (MC). The MICRO score is defined as a weighted average of the scores for *moments* of different lengths, where the weight is proportional to the total number of test-moments of that size. The full breakdown of results is available in appendix D.

Figure 1a shows MICRO MSPC for the three models and the baseline. The first observation is that all models perform significantly better than the baseline. Recall that the baseline is essentially remembering the *moments* that it has observed at training, therefore it is natural that as we increase the number of training sequences its performance approaches that of the learned models. Figure 1b shows the analogous results when MSPC is computed over unseen *moments*, the baseline in this case is undefined since by definition the expectation over all unseen *moments* will be zero. Still the models seem to be learning to rank unseen *moments*, and therefore they are making proper generalizations.

However, one obvious observation is that the MSPC is not very high in absolute terms (appendix D tables, both in the all and unseen scenarios). Looking at the absolute value of the MSPC might be misleading because we are modeling a sparse sequence classification task. In other words, the gold expectation for most of the *moments* in the domain is zero and in this case the MSPC metric might be too harsh. Thus, as described in Section 3.1, we turn our attention to MR.

The MR metric reflects the model's ability to predict the non-zero *moments* of the distribution and as shown in Figure 1c all models learn to do this relatively well. This is also true for the generalization setting (Figure 1d) in which models are forced to make predictions over unseen *moments*.

To gain more insight into the distributions induced by the models, another way of breaking down the MSPC metric is to focus on how well a model ranks the non-zero *moments* of the gold distribution. That is, in this case, we tell the model which *moments* are non-zero and let the model rank them. Figure 1e shows MSPCP. We can see that all models learn to rank the *moments* of the target class and

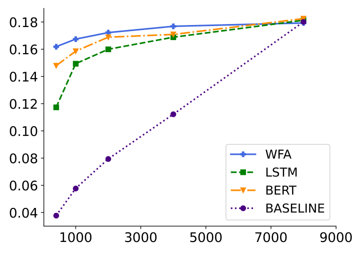

(a) MICRO MSPC

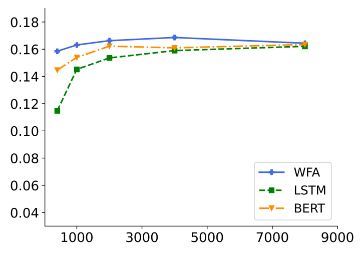

(b) MICRO MSPC-U

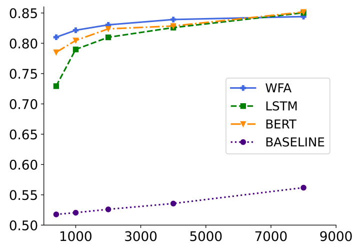

(c) MICRO MR

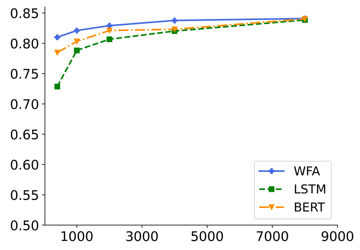

(d) MICRO MR-U

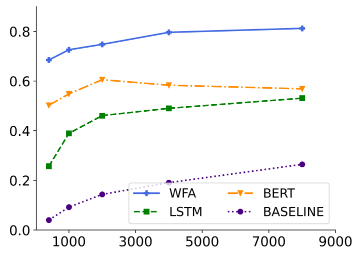

(e) MICRO MSPCP

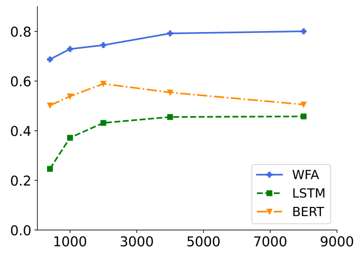

(f) MICRO MSPCP-U

Figure 1: MICRO MSPC, MR and MSPCP results

this also holds true for unseen *moments* (Figure 1f). In this evaluation scenario, the WFA seems to be better than the other two models. This is most likely due to the difference between the loss function minimized by the WFA and the loss functions minimized by the LSTM and BERT models. The WFA classifier is defined as an ensemble of class specific models, and therefore it is explicitly modeling the class distributions.

Finally we also explored correlations between different models by computing pairwise Spearman correlation between the model's predictions. We found out that the correlation is high for shorter *moments* and that it decreases significantly with longer ones. Regarding pairwise associations, LSTM and BERT show a higher level of agreement, while the WFA is more correlated to BERT overall.

5 Conclusion

In this paper we presented a novel evaluation framework for comparing sequence classification models and for testing the extent to which they can implicitly learn the target distribution. Our results comparing three different deep-learning models suggest that the models have the ability to learn the underlying distribution. They also suggest that despite significant differences in the architectures and even in the loss functions (i.e. for the WFA), their performance is comparable. The goal of this paper was to develop a simple way to gain insights into what is actually been learned by a given sequence classifier. But the evaluation approach itself also suggests ways in which we could exploit unlabeled data to obtain better calibrated sequence classifiers, future work should explore this possibility.

Acknowledgments and Disclosure of Funding

The authors gratefully acknowledge the computer resources at ARTEMISA, funded by the European Union ERDF and Comunitat Valenciana as well as the technical support provided by the Instituto de Física Corpuscular, IFIC (CSIC-UV). This work is supported by the European Research Council (ERC) under the European Union's Horizon 2020 research and innovation program (grant agreement No.853459).

References

Y. Bai, J. Mei, A. L. Yuille, and C. Xie. Are transformers more robust than cnns? *CoRR*, abs/2111.05464, 2021. URL `https://arxiv.org/abs/2111.05464`.

B. Balle, X. Carreras, F. M. Luque, and A. Quattoni. Spectral learning of weighted automata. *Machine Learning*, 96(1):33–63, Jul 2014. ISSN 1573-0565. doi: 10.1007/s10994-013-5416-x. URL `https://doi.org/10.1007/s10994-013-5416-x`.

M. L. Bileschi, D. Belanger, D. Bryant, T. Sanderson, B. Carter, D. Sculley, M. A. DePristo, and L. J. Colwell. Using deep learning to annotate the protein universe. *bioRxiv*, 2019. doi: 10.1101/626507. URL `https://www.biorxiv.org/content/early/2019/05/04/626507`.

N. De Cao, W. Aziz, and I. Titov. Block neural autoregressive flow. In R. P. Adams and V. Gogate, editors, *Proceedings of The 35th Uncertainty in Artificial Intelligence Conference*, volume 115 of *Proceedings of Machine Learning Research*, pages 1263–1273. PMLR, 22–25 Jul 2020. URL `https://proceedings.mlr.press/v115/de-cao20a.html`.

S. Desai and G. Durrett. Calibration of pre-trained transformers. In *Proceedings of the 2020 Conference on Empirical Methods in Natural Language Processing (EMNLP)*, pages 295–302, Online, Nov. 2020. Association for Computational Linguistics. doi: 10.18653/v1/2020.emnlp-main.21. URL `https://aclanthology.org/2020.emnlp-main.21`.

J. Devlin, M.-W. Chang, K. Lee, and K. Toutanova. BERT: Pre-training of deep bidirectional transformers for language understanding. In *Proceedings of the 2019 Conference of the North American Chapter of the Association for Computational Linguistics: Human Language Technologies, Volume 1 (Long and Short Papers)*, pages 4171–4186, Minneapolis, Minnesota, June 2019. Association for Computational Linguistics. doi: 10.18653/v1/N19-1423. URL `https://aclanthology.org/N19-1423`.

C. Durkan, A. Bekasov, I. Murray, and G. Papamakarios. Neural spline flows. In H. Wallach, H. Larochelle, A. Beygelzimer, F. d'Alché-Buc, E. Fox, and R. Garnett, editors, *Advances in Neural Information Processing Systems*, volume 32. Curran Associates, Inc., 2019. URL `https://proceedings.neurips.cc/paper/2019/file/7ac71d433f282034e088473244df8c02-Paper.pdf`.

S. El-Gebali, J. Mistry, A. Bateman, S. R. Eddy, A. Luciani, S. C. Potter, M. Qureshi, L. J. Richardson, G. A. Salazar, A. Smart, E. L. Sonnhammer, L. Hirsh, L. Paladin, D. Piovesan, S. C. Tosatto, and R. D. Finn. The Pfam protein families database in 2019. *Nucleic Acids Research*, 47(D1): D427–D432, 10 2018. ISSN 0305-1048. doi: 10.1093/nar/gky995. URL `https://doi.org/10.1093/nar/gky995`.

E. Eskin. *Sparse sequence modeling with applications to computational biology and intrusion detection*. Columbia University, 2002.

R. Fakoor, P. Chaudhari, J. Mueller, and A. J. Smola. Trade: Transformers for density estimation. *CoRR*, abs/2004.02441, 2020. URL `https://arxiv.org/abs/2004.02441`.

C. Guo, G. Pleiss, Y. Sun, and K. Q. Weinberger. On calibration of modern neural networks. In *Proceedings of the 34th International Conference on Machine Learning - Volume 70*, ICML'17, page 1321–1330. JMLR.org, 2017.

S. Hochreiter and J. Schmidhuber. Long Short-Term Memory. *Neural Computation*, 9(8):1735–1780, 11 1997. ISSN 0899-7667. doi: 10.1162/neco.1997.9.8.1735. URL `https://doi.org/10.1162/neco.1997.9.8.1735`.

R. Józefowicz, O. Vinyals, M. Schuster, N. Shazeer, and Y. Wu. Exploring the limits of language modeling. *CoRR*, abs/1602.02410, 2016. URL `http://arxiv.org/abs/1602.02410`.

S. Karita, N. Chen, T. Hayashi, T. Hori, H. Inaguma, Z. Jiang, M. Someki, N. E. Y. Soplin, R. Yamamoto, X. Wang, S. Watanabe, T. Yoshimura, and W. Zhang. A comparative study on transformer vs rnn in speech applications. In *2019 IEEE Automatic Speech Recognition and Understanding Workshop (ASRU)*, pages 449–456, 2019. doi: 10.1109/ASRU46091.2019.9003750.

D. Kingma and J. Ba. Adam: A method for stochastic optimization. *International Conference on Learning Representations*, 12 2014.

A. Kolesnikov, A. Dosovitskiy, D. Weissenborn, G. Heigold, J. Uszkoreit, L. Beyer, M. Minderer, M. Dehghani, N. Houlsby, S. Gelly, T. Unterthiner, and X. Zhai. An image is worth 16x16 words: Transformers for image recognition at scale. 2021.

A. Kumar and S. Sarawagi. Calibration of encoder decoder models for neural machine translation. *CoRR*, abs/1903.00802, 2019. URL `http://arxiv.org/abs/1903.00802`.

S. M. Lakew, M. Cettolo, and M. Federico. A comparison of transformer and recurrent neural networks on multilingual neural machine translation. In *Proceedings of the 27th International Conference on Computational Linguistics*, pages 641–652, Santa Fe, New Mexico, USA, Aug. 2018. Association for Computational Linguistics. URL `https://aclanthology.org/C18-1054`.

A. Niculescu-Mizil and R. Caruana. Predicting good probabilities with supervised learning. In *Proceedings of the 22nd International Conference on Machine Learning*, ICML '05, page 625–632, New York, NY, USA, 2005. Association for Computing Machinery. ISBN 1595931805. doi: 10.1145/1102351.1102430. URL `https://doi.org/10.1145/1102351.1102430`.

J. B. Oliva, A. Dubey, M. Zaheer, B. Póczos, R. Salakhutdinov, E. P. Xing, and J. Schneider. Transformation autoregressive networks, 2018.

F. Pinto, P. Torr, and P. K. Dokania. Are vision transformers always more robust than convolutional neural networks? In *NeurIPS 2021 Workshop on Distribution Shifts: Connecting Methods and Applications*, 2021. URL `https://openreview.net/forum?id=CSXa8LJMttt`.

A. Quattoni and X. Carreras. Interpolated spectral NGram language models. In *Proceedings of the 57th Annual Meeting of the Association for Computational Linguistics*, pages 5926–5930, Florence, Italy, July 2019. Association for Computational Linguistics. doi: 10.18653/v1/P19-1594. URL `https://aclanthology.org/P19-1594`.

A. Quattoni and X. Carreras. A comparison between CNNs and WFAs for sequence classification. In *Proceedings of SustaiNLP: Workshop on Simple and Efficient Natural Language Processing*, pages 159–163, Online, Nov. 2020. Association for Computational Linguistics. doi: 10.18653/v1/2020.sustainlp-1.21. URL `https://aclanthology.org/2020.sustainlp-1.21`.

A. Quattoni, X. Carreras, and M. Gallé. A Maximum Matching Algorithm for Basis Selection in Spectral Learning. In A. Singh and J. Zhu, editors, *Proceedings of the 20th International Conference on Artificial Intelligence and Statistics*, volume 54 of *Proceedings of Machine Learning Research*, pages 1477–1485. PMLR, 20–22 Apr 2017. URL `https://proceedings.mlr.press/v54/quattoni17a.html`.

G. Rabusseau, T. Li, and D. Precup. Connecting weighted automata and recurrent neural networks through spectral learning. In K. Chaudhuri and M. Sugiyama, editors, *Proceedings of Machine Learning Research*, volume 89 of *Proceedings of Machine Learning Research*, pages 1630–1639. PMLR, 16–18 Apr 2019. URL `http://proceedings.mlr.press/v89/rabusseau19a.html`.

B. Szalkai and V. Grolmusz. Near perfect protein multi-label classification with deep neural networks. *Methods*, 132:50–56, 2018.

B. Uria, M.-A. Côté, K. Gregor, I. Murray, and H. Larochelle. Neural autoregressive distribution estimation. *J. Mach. Learn. Res.*, 17(1):7184–7220, jan 2016. ISSN 1532-4435.

W. Yin, K. Kann, M. Yu, and H. Schütze. Comparative study of CNN and RNN for natural language processing. *CoRR*, abs/1702.01923, 2017. URL `http://arxiv.org/abs/1702.01923`.

A Optimization Details

For each of our training sets $T^m = \{(x^{(1)}, y^{(1)}), \ldots, (x^{(m)}, y^{(m)})\}$ we train a new model and validate the parameters independently. We use a 2 layer LSTM and we validate all parameters such as the dimension of the hidden state, of the embeddings and the learning rate with a grid search evaluated on the validation data. We proceed analogously for the BERT parameters, note that we use the *bert-base* model.

We use Adam [Kingma and Ba, 2014] as optimizer employing the standard cross entropy loss function. For both LSTM and BERT we train 5 models with different starting random seeds for each training set and we report the average of the results.

Table 1: Training time and minimum number of parameters to fully compress 8000 sequences.

	Training time (s)	**# of parameters**
WFA	67	1.15×10^5
LSTM	63	1×10^6
BERT	305	1.1×10^8

For the WFA model the only parameter that we need to validate is the number of states k. Besides, as there are no randomly initialized parameters and the training is not stochastic, we don't need to perform multiple runs with multiple seeds. The WFA is trained using the spectral learning method. For a detailed and comprehensive explanation of the training method the reader is referred to Balle et al. [2014]. Furthermore, we employ the scalability techniques described in Quattoni et al. [2017].

LSTM and BERT models were trained on a single GPU while the WFA, for which the bottleneck is computing a singular value decomposition of a large sparse matrix, was trained on a CPU. To give an idea of the relative size of each model, we computed the minimum number of parameters for which the models were able to achieve perfect classification on our biggest training set. We report the numbers in Table 1.

B Data

Here we presents some statistics about the data that we have generated. There are a total of 23 amino acid symbols.

Table 2: Dataset statistics.

	# of sequences	**% wrt $\lvert \cup_n Z_n \rvert$**
$\lvert \cup_n Z_n \rvert$	1.8×10^6	-
$\lvert Z_1^Y \rvert$	2×10^1	86.96%
$\lvert Z_2^Y \rvert$	3.9×10^2	86.70%
$\lvert Z_3^Y \rvert$	4.1×10^3	49.89%
$\lvert Z_4^Y \rvert$	1.5×10^4	10.00%
$\lvert Z_5^Y \rvert$	2.8×10^4	1.68%

C Models correlation

Here we show a figure displaying the pairwise Spearman correlation between the model's predictions. N_i stands for the different ngram lengths.

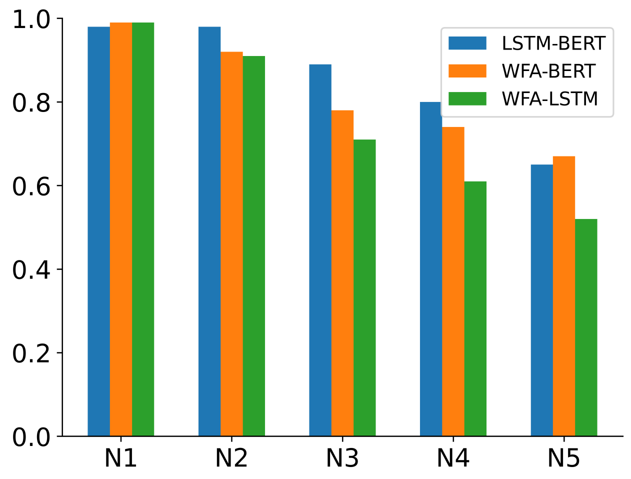

Figure 2: MSPC between models.

D Result Tables

Table 3: MSPC, 400 Training Sequences.

	WFA	**LSTM**	**BERT**	**BASELINE**
N1	0.92878	0.87715	0.88803	0.88812
N2	0.86161	0.7269	0.81566	0.62104
N3	0.64555	0.41444	0.57328	0.16744
N4	0.34245	0.22023	0.30406	0.051655
N5	0.14245	0.10607	0.13102	0.03562
MICRO	0.16185	0.1173	0.14786	0.037732

Table 4: MSPC, 1000 Training Sequences.

	WFA	**LSTM**	**BERT**	**BASELINE**
N1	0.94362	0.93947	0.95351	0.90198
N2	0.88806	0.7933	0.86798	0.75504
N3	0.67164	0.51563	0.628	0.26579
N4	0.3531	0.29955	0.33486	0.086673
N5	0.14741	0.13336	0.13959	0.053745
MICRO	0.1674	0.14934	0.15853	0.05768

Table 5: MSPC, 2000 Training Sequences.

	WFA	**LSTM**	**BERT**	**BASELINE**
N1	0.96439	0.95964	0.94995	0.86733
N2	0.92286	0.87423	0.90971	0.75083
N3	0.70414	0.58983	0.68951	0.34454
N4	0.36564	0.3234	0.36066	0.11984
N5	0.15135	0.1424	0.14818	0.07408
MICRO	0.1722	0.15994	0.16882	0.079362

Table 6: MSPC, 4000 Training Sequences.

	WFA	**LSTM**	**BERT**	**BASELINE**
N1	0.97824	0.96855	0.96439	0.92673
N2	0.94558	0.8781	0.92219	0.79916
N3	0.73057	0.63392	0.68747	0.442
N4	0.37522	0.34892	0.35885	0.16727
N5	0.15539	0.14952	0.15057	0.10524
MICRO	0.17682	0.16879	0.17084	0.1122

Table 7: MSPC, 8000 Training Sequences.

	WFA	**LSTM**	**BERT**	**BASELINE**
N1	0.98714	0.98398	0.98022	0.94554
N2	0.94925	0.92542	0.93935	0.82521
N3	0.73837	0.69595	0.72027	0.55846
N4	0.37987	0.37275	0.38072	0.25477
N5	0.15761	0.16066	0.16111	0.17104
MICRO	0.17927	0.18125	0.18245	0.18006

Table 8: MR, 400 Training Sequences.

	WFA	**LSTM**	**BERT**	**BASELINE**
N4	0.78962	0.68841	0.75878	0.52947
N5	0.81186	0.73307	0.7875	0.51656
MICRO	0.80996	0.72927	0.78505	0.51765

Table 9: MR, 1000 Training Sequences.

	WFA	**LSTM**	**BERT**	**BASELINE**
N4	0.79955	0.75561	0.78494	0.53438
N5	0.82346	0.793	0.80632	0.51921
MICRO	0.82143	0.78982	0.8045	0.5205

Table 10: MR, 2000 Training Sequences.

	WFA	**LSTM**	**BERT**	**BASELINE**
N4	0.81061	0.77585	0.80705	0.54377
N5	0.83217	0.81294	0.82522	0.52434
MICRO	0.83034	0.80979	0.82368	0.526

Table 11: MR, 4000 Training Sequences.

	WFA	**LSTM**	**BERT**	**BASELINE**
N4	0.81873	0.79771	0.80568	0.55984
N5	0.84102	0.82841	0.83056	0.53338
MICRO	0.83913	0.8258	0.82844	0.53563

Table 12: MR, 8000 Training Sequences.

	WFA	**LSTM**	**BERT**	**BASELINE**
N4	0.82277	0.81864	0.82526	0.59726
N5	0.84592	0.85317	0.85399	0.55846
MICRO	0.84395	0.85023	0.85155	0.56176

Table 13: MSPCP, 400 Training Sequences.

	WFA	**LSTM**	**BERT**	**BASELINE**
N1	0.89774	0.81564	0.83128	0.83008
N2	0.83119	0.6226	0.7294	0.55278
N3	0.6639	0.33845	0.51782	0.1582
N4	0.6367	0.23165	0.44983	0.053211
N5	0.71182	0.25286	0.52513	0.0077381
MICRO	0.68458	0.25665	0.50207	0.040077

Table 14: MSPCP 1000, Training Sequences.

	WFA	**LSTM**	**BERT**	**BASELINE**
N1	0.91579	0.90947	0.93083	0.85113
N2	0.84449	0.71795	0.81302	0.67625
N3	0.69214	0.48918	0.61035	0.26223
N4	0.66321	0.38853	0.51871	0.12028
N5	0.76345	0.36944	0.55099	0.042548
MICRO	0.7258	0.38895	0.54801	0.091939

Table 15: MSPCP, 2000 Training Sequences.

	WFA	**LSTM**	**BERT**	**BASELINE**
N1	0.94737	0.94015	0.92541	0.7985
N2	0.89145	0.82017	0.86927	0.64694
N3	0.72948	0.57631	0.66934	0.35078
N4	0.69176	0.46408	0.57831	0.18212
N5	0.77876	0.43644	0.60665	0.083977
MICRO	0.74752	0.4607	0.60521	0.14338

Table 16: MSPCP, 4000 Training Sequences.

	WFA	**LSTM**	**BERT**	**BASELINE**
N1	0.96842	0.95368	0.94737	0.88872
N2	0.92282	0.83142	0.88642	0.70724
N3	0.77011	0.58983	0.67558	0.46542
N4	0.73517	0.48084	0.56523	0.24313
N5	0.83144	0.47518	0.57467	0.11361
MICRO	0.79601	0.48997	0.58302	0.19071

Table 17: MSPCP, 8000 Training Sequences.

	WFA	**LSTM**	**BERT**	**BASELINE**
N1	0.98195	0.97714	0.97143	0.91729
N2	0.93024	0.90049	0.91239	0.73807
N3	0.78783	0.67781	0.70733	0.59942
N4	0.7477	0.53759	0.56915	0.35323
N5	0.8491	0.50004	0.54256	0.1588
MICRO	0.81193	0.53088	0.56849	0.2643

Table 18: MSPC-U, 400 Training Sequences.

	WFA	**LSTM**	**BERT**
N2	0.77232	0.73303	0.81822
N3	0.63313	0.40291	0.56004
N4	0.34065	0.2175	0.3016
N5	0.14201	0.10539	0.13042
MICRO	0.1585	0.11474	0.14464

Table 19: MSPC-U, 1000 Training Sequences.

	WFA	**LSTM**	**BERT**
N2	0.81324	0.82896	0.83926
N3	0.64174	0.48128	0.59383
N4	0.34826	0.29307	0.32861
N5	0.14637	0.13186	0.13814
MICRO	0.16311	0.14516	0.15393

Table 20: MSPC-U, 2000 Training Sequences.

	WFA	**LSTM**	**BERT**
N2	0.8269	0.83715	0.84263
N3	0.65265	0.53285	0.63791
N4	0.35574	0.31071	0.349
N5	0.14912	0.13942	0.14534
MICRO	0.16625	0.15358	0.16222

Table 21: MSPC-U, 4000 Training Sequences.

	WFA	**LSTM**	**BERT**
N2	0.76113	0.71213	0.75573
N3	0.64381	0.53365	0.59127
N4	0.3578	0.32639	0.33669
N5	0.15151	0.14394	0.14514
MICRO	0.1686	0.15897	0.16098

Table 22: MSPC-U, 8000 Training Sequences.

	WFA	**LSTM**	**BERT**
N2	0.55257	0.45058	0.54054
N3	0.5661	0.49899	0.53307
N4	0.34073	0.32207	0.33099
N5	0.14853	0.14779	0.14838
MICRO	0.16437	0.16211	0.16341

Table 23: MR-U, 400 Training Sequences.

	WFA	**LSTM**	**BERT**
N4	0.78938	0.68689	0.75781
N5	0.81158	0.73209	0.7868
MICRO	0.80984	0.72854	0.78452

Table 24: MR-U, 1000 Training Sequences.

	WFA	**LSTM**	**BERT**
N4	0.79892	0.753	0.78288
N5	0.82284	0.79121	0.80471
MICRO	0.82096	0.7882	0.803

Table 25: MR-U, 2000 Training Sequences.

	WFA	**LSTM**	**BERT**
N4	0.80935	0.77132	0.80411
N5	0.83072	0.80961	0.82234
MICRO	0.82903	0.8066	0.82091

Table 26: MR-U, 4000 Training Sequences.

	WFA	**LSTM**	**BERT**
N4	0.81769	0.79101	0.79967
N5	0.83928	0.82256	0.82509
MICRO	0.83758	0.82008	0.82309

Table 27: MR-U, 8000 Training Sequences.

	WFA	**LSTM**	**BERT**
N4	0.8205	0.80457	0.81277
N5	0.8425	0.84127	0.84245
MICRO	0.84077	0.83838	0.84012

Table 28: MSPCP-U, 400 Training Sequences.

	WFA	**LSTM**	**BERT**
N2	0.70856	0.54879	0.62302
N3	0.64968	0.31778	0.49905
N4	0.63467	0.22759	0.44711
N5	0.71121	0.25239	0.52548
MICRO	0.68721	0.24644	0.50169

Table 29: MSPCP-U, 1000 Training Sequences.

	WFA	**LSTM**	**BERT**
N2	0.56343	0.63362	0.61802
N3	0.66231	0.43854	0.56343
N4	0.65681	0.37763	0.5092
N5	0.7621	0.36656	0.54989
MICRO	0.72875	0.37139	0.53812

Table 30: MSPCP-U, 2000 Training Sequences.

	WFA	**LSTM**	**BERT**
N2	0.52016	0.65202	0.64873
N3	0.67633	0.49721	0.60039
N4	0.67863	0.43764	0.55913
N5	0.77518	0.42648	0.60156
MICRO	0.74444	0.43131	0.58896

Table 31: MSPCP-U 4000 Training Sequences.

	WFA	**LSTM**	**BERT**
N2	0.52822	0.58149	0.54327
N3	0.69234	0.45822	0.56041
N4	0.71764	0.44072	0.53155
N5	0.82694	0.46119	0.56332
MICRO	0.79166	0.45506	0.55384

Table 32: MSPCP-U, 8000 Training Sequences.

	WFA	**LSTM**	**BERT**
N2	0.81084	0.59462	0.24505
N3	0.6507	0.46172	0.48333
N4	0.71584	0.4504	0.49123
N5	0.84148	0.46038	0.51201
MICRO	0.80016	0.45745	0.50523